



A Formyl Chromone Based Schiff Base Derivative: An Efficient Colorimetric and Fluorescence Chemosensor for the Selective Detection of Hg²⁺ Ions

Soumya Ranjan Kar¹ · Pragyana Parimita Dash¹ · Sankalpa Narayan Panda¹ · Patitapaban Mohanty¹ · Debasis Mohanty² · Aruna Kumar Barick¹ · Suban Kumar Sahoo³ · Priyaranjan Mohapatra¹ · Bigyan Ranjan Jali¹

Received: 1 October 2023 / Accepted: 6 November 2023

© The Author(s), under exclusive licence to Springer Science+Business Media, LLC, part of Springer Nature 2024, corrected publication 2024

Abstract

A novel chromone-based Schiff base **L** was designed and synthesized by condensing an equimolar amount of 3-formyl chromone and 2,4-dinitro phenyl hydrazine. Schiff base **L** was developed as a potent colorimetric and fluorescent molecular probe to recognize Hg²⁺ ions over other competitive metal ions. In the presence of Hg²⁺, Schiff base **L** displays a naked-eye detectable color change under day and UV_{365 nm} light. Various UV-Vis and fluorescence studies of **L** were performed in the absence and presence of Hg²⁺ to determine the sensitivity and the sensing mechanism. With high selectivity and specificity, the detection limit and association constant of **L** for Hg²⁺ were estimated at 1.87 μM and 1.234 × 10⁷ M⁻¹, respectively. The developed sensor **L** was applied to real soil samples for the detection of Hg²⁺.

Keywords Formyl chromone · Schiff base · Fluorescent and colorimetric sensor · Hg²⁺

Introduction

Schiff bases are widely employed for the design of chromofluorogenic chemosensors due to their potent photophysical characteristics and attractive coordination behavior [1]. Schiff base derivatives are well-known for their antibacterial [2], antifungal [3], anticancer [4], antitumor [5] and cytotoxicity characteristics [6]. Schiff bases act as effective corrosion inhibitors and are also utilized as catalysts in a variety of chemical processes [7]. Schiff base derivatives are employed as active binding receptors to bind various metal ions with the imine-N atom [8]. During complex formation, the electron density is transferred from the imine group to the metal

ion [9]. The complexation-induced ligand to metal charge transfer (LMCT) resulted naked-eye detectable color and spectral changes that allowed on-site detection of metal ion [10]. Literature also revealed that Schiff base derived chromofluorogenic chemosensors have gained significant attention in the last few decades due to their potential applications in environmental, biological and industrial processes [11].

Mercury is one of the most toxic heavy metals in the human body [12]. The USEAP and WHO have recommended a permissible limit of 2 ppb of Hg²⁺ concentration in drinking water [13]. Some microbes turn various forms of mercury into the potent poison methyl mercury [14]. As a non-biodegradable contaminant, mercury can harm the kidney and brain as well as cause serious health conditions like Minamata disease [15]. It may also affect the immune system and the heart [16], resulting in a number of illnesses, including memory loss, the birth of abnormal offspring, a drop in muscular strength, and a decrease in the body's overall immunity [17]. So, the detection of trace amounts of mercury is so necessary now a day. The fluorescence detection method over other methods has piqued the interest of scientists due to its significant advantages [18], such as real-time detection, high sensitivity [19], high selectivity and non-invasive features [20]. Many attempts have already

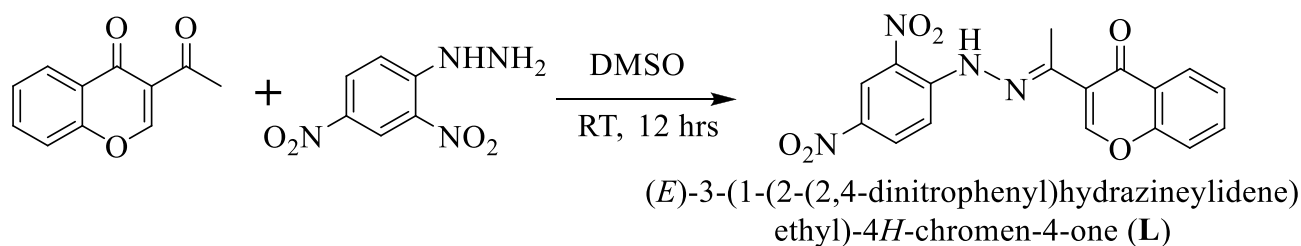
✉ Priyaranjan Mohapatra
priya46418@gmail.com

✉ Bigyan Ranjan Jali
bigyan.Jali7@gmail.com

¹ Department of Chemistry, Veer Surendra Sai University of Technology, Burla, Sambalpur, Odisha, India

² Dhenkanal (Auto) College, Dhenkanal, Odisha, India

³ Department of Chemistry, Sardar Vallabhbhai National Institute of Technology, Surat 395007, India



Scheme 1 Synthesis of (E)-3-(1-(2-(2,4-dinitrophenyl)hydrazineylidene)ethyl)-4 H-chromen-4-one (**L**)

been made to synthesize fluorescent sensors that could recognize Hg^{2+} ions by deprotonating thiols [21], ring opening of rhodamine derivatives [22], cyclizing [23], ring opening of thiourea derivatives [24] and, other processes [25]. However, these fluorescent sensors have a number of drawbacks, including a convoluted structure and arduous chemical synthesis, which limit their practical use in environmental monitoring and biological tests [26]. Considering the above facts, this manuscript introduced an easy-to-synthesize chromone-derived Schiff-base (E)-3-(1-(2-(2,4-dinitrophenyl)hydrazineylidene)ethyl)-4 H-chromen-4-one (**L**) (Scheme 1) for the selective detection of Hg^{2+} . The receptor **L** exhibited Hg^{2+} selective turn-on fluorescence at 544 nm in DMSO.

Experimental

Materials and Instruments

The chemicals (3-formyl chromone and 2,4-dinitrophenyl hydrazine) and solvents were obtained from Sigma-Aldrich. The chloride salts of Na^+ , Li^+ , Mn^{2+} , Cr^{2+} , Ni^{2+} , Ca^{2+} , Mg^{2+} , K^+ , Co^{2+} , Cu^{2+} , Zn^{2+} , Al^{3+} and Hg^{2+} and sulfate salt of Fe^{2+} were obtained from CDH. UV-Visible spectra were recorded in the wavelength region of 200–800 nm. The FTIR spectrum was recorded using a Bruker Alpha ECO-ATR instrument over a wide range of wave number of 4000 to 400 cm^{-1} . A Perkin-Elmer LS-55 fluorescence spectrophotometer was used to record the fluorescence spectrum with slit width of 5.0 nm. The HRMS data of the receptor was recorded from a SCIX-QTOF Mass spectrometer in DMSO solvent. Using ZEN-3690 Zetasizer device of Malvern Panalytical Ltd., Hyogo, Japan, the hydrodynamic diameters were recorded. All the experiments were performed at ambient temperature. Double distilled water was utilized in all spectral experiments.

Synthesis and Characterization

A formyl chromone-based Schiff base ligand, (E)-3-(1-(2-(2,4-dinitrophenyl)hydrazineylidene)ethyl)-4 H-chromen-4-one (**L**) was prepared by the 1:1 addition of 2,4-dinitrophenyl

hydrazine and 3-acetyl-4 H-chromen-4-one in ethanol based on a previously reported method (Scheme 1) [27].

UV-Vis and Fluorescence Studies

The standard solutions of several metal salts (10^{-5} M) were made in deionized water. The standard solution of **L** (10^{-5} M) was made in a solvent of DMSO. For the UV-Vis and fluorescence titration studies, 2.0 mL solution of **L** was filled into quartz optical cells with a 1 cm path length. Using a micropipette, required amounts of metal ions were added and spectra were recorded to examine the selectivity, specificity and sensitivity. The spectra were captured within 1 min of the metal salts being added. All measurements are performed at room temperature. For fluorescence measurement of **L** ($\lambda_{\text{ex}} = 410/\lambda_{\text{em}} = 544$ nm), the widths of the emission and excitation slits were fixed at 5 nm. Using the fluorescence titration data, the limit of detection (LOD) was calculated using the IUPAC-certified formula, $\text{LOD} = 3\sigma/\text{slope}$ [28]. Here σ stands for the standard deviation of a free sample.

The Benesi-Hildebrand plot is used to determine the association constant and association stoichiometry from the fluorescence titrations [29]. The Benesi-Hildebrand equation [30] for a 1:n complex type comprising a ligand and M^{n+} is given as follows.

$$\frac{1}{F - F_0} = \frac{1}{F_\infty - F_0} + \frac{1}{K[\text{M}^{n+}]^n \left(\frac{1}{F_\infty - F_0} \right)} \quad (1)$$

where, F and F_0 are emissions of receptor **L** in the absence and presence of Hg^{2+} ions. F_∞ is the maximum fluorescence intensity of **L** with metal ions at saturation. $[\text{M}^{n+}]$ is the concentration of Hg^{2+} ions and K is the association constant.

Results and Discussion

The azomethine group of Schiff bases serves as an active interaction site for metal ions due to its chelating nature [31]. In the above aspect, a novel chromone-based Schiff base **L** is designed and synthesized in a 1:1 addition of 2,4-dinitrophenyl hydrazine and 3-acetyl-4 H-chromen-4-one in DMSO

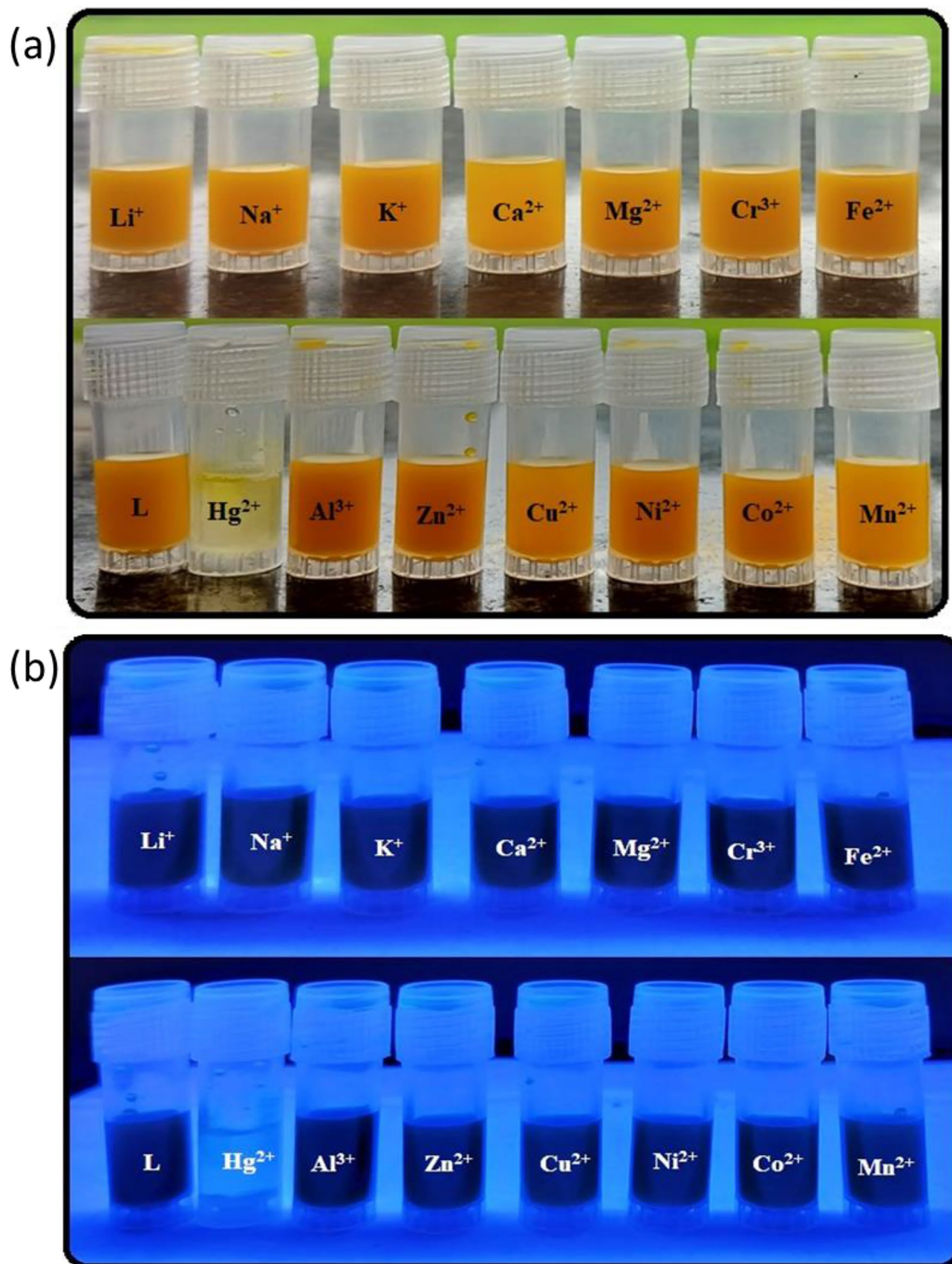
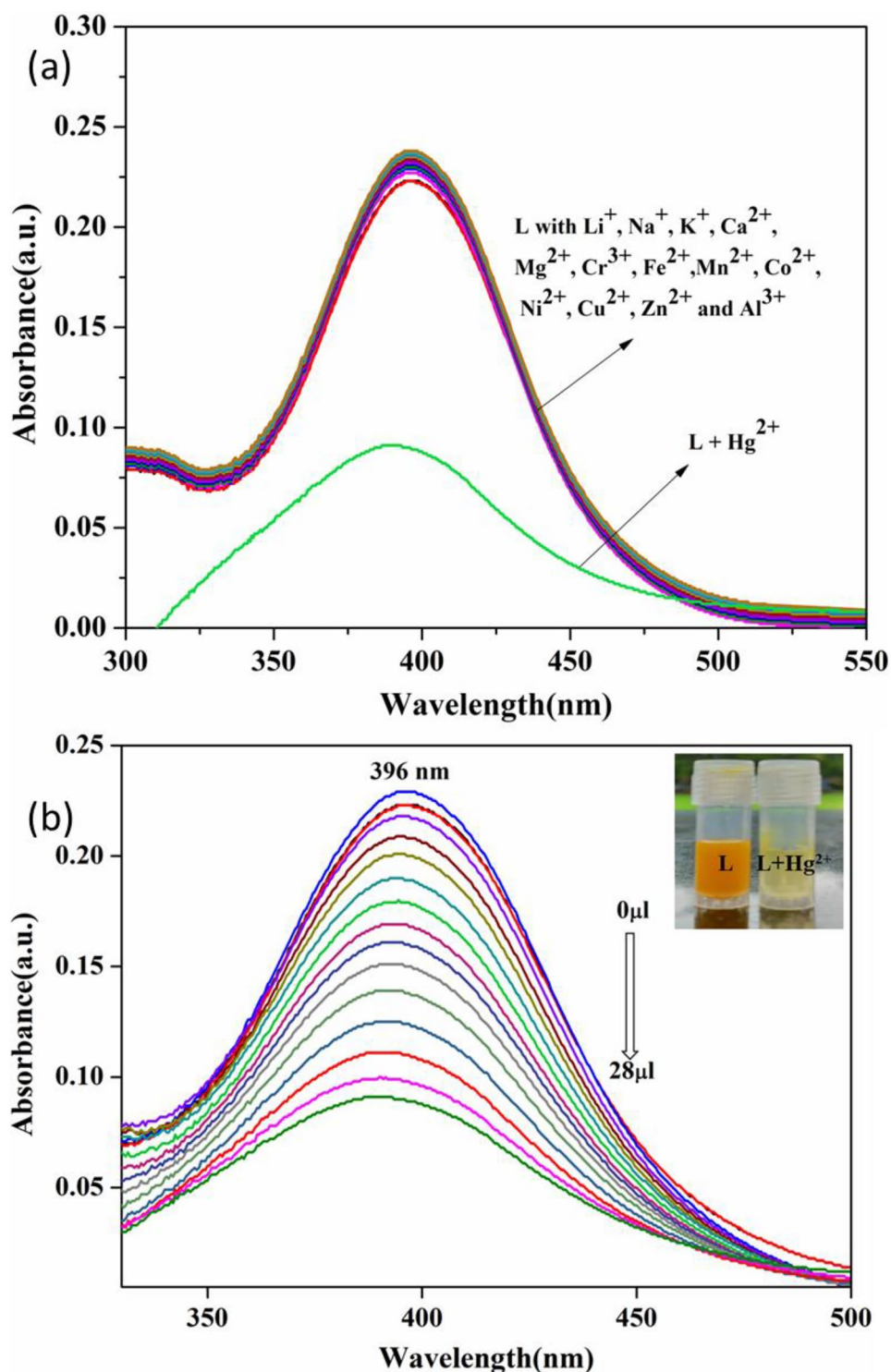


Fig. 1 Colorimetric changes of L (10^{-5} M, DMSO) in the presence of several metal ions (10^{-5} M): under day light (a) and UV lamp at 365 nm (b)

Fig. 2 **a** UV-Vis absorption spectra of **L** (2000 μL , 10^{-5} M) in DMSO upon the incorporation of various metal ions (2 μL in each aliquot); **b** UV-vis absorption intensity of **L** that changes when Hg^{2+} ions are added gradually (0–28 μL , 10^{-5} M)



(Scheme 1). After characterization, the selectivity and sensitivity of **L** towards Hg^{2+} , among other competitive metal ions were analyzed through various spectrophotometric analyses like UV-Vis, fluorescence and dynamic scattering analysis (DLS) [32].

Colorimetric Analysis

To analyze the potential use of the synthesized chromone derivative **L** as a colorimetric chemosensor, the colorimetric studies are analyzed by adding various metal ions [33]. The

DMSO solution of **L** was interacted individually with different metal ions, such as Na^+ , Mn^{2+} , Li^+ , Cr^{3+} , Fe^{2+} , Ni^{2+} , Ca^{2+} , Mg^{2+} , K^+ , Co^{2+} , Cu^{2+} , Zn^{2+} , Al^{3+} and Hg^{2+} , no such color change response was observed except for Hg^{2+} . The incorporation of Hg^{2+} ions into the orange-colored solution of **L** results in a change in color to light yellow, which is visible to the naked-eye (Fig. 1a). Also, the non-fluorescent **L** changed to light blue fluorescent in the presence of Hg^{2+} when irradiated with $\text{UV}_{365\text{ nm}}$ light (Fig. 1b).

UV-Vis Absorption Spectral Studies

The sensing capabilities of **L** towards metal ions including Na^+ , Mn^{2+} , Li^+ , Cr^{3+} , Fe^{2+} , Ni^{2+} , Ca^{2+} , Mg^{2+} , K^+ , Co^{2+} , Cu^{2+} , Zn^{2+} , Al^{3+} and Hg^{2+} were studied in DMSO medium by UV-Vis absorption spectroscopy [34]. It was astonishing

to know that the addition of distinct metal ions to the DMSO solution of **L** results in an alteration in absorption intensity in the presence of Hg^{2+} (Fig. 2a). The absorption spectra of **L** in DMSO solution displayed a strong absorbance peak at 396 nm. The absorption peak of **L** at 396 nm was due to the $n\text{-}\pi^*$ transition between the lone pair electron of the N-atom and the aromatic π electron of the aromatic ring. The incorporation of Hg^{2+} into the DMSO solution of **L** results in a decrease in absorption intensity at 396 nm. In the case of other metal ions except Hg^{2+} , no such considerable alteration in absorption spectra was observed.

The incremental addition of Hg^{2+} to the DMSO solution of **L** resulted in a gradual decrease in the absorption intensity at 396 nm (Fig. 2b). The change in spectral behavior is associated with a slight blue shift of the absorption peak from 396 nm to 389 nm with a distinct color alteration of orange color to pale yellow which is discernible in the naked-eye

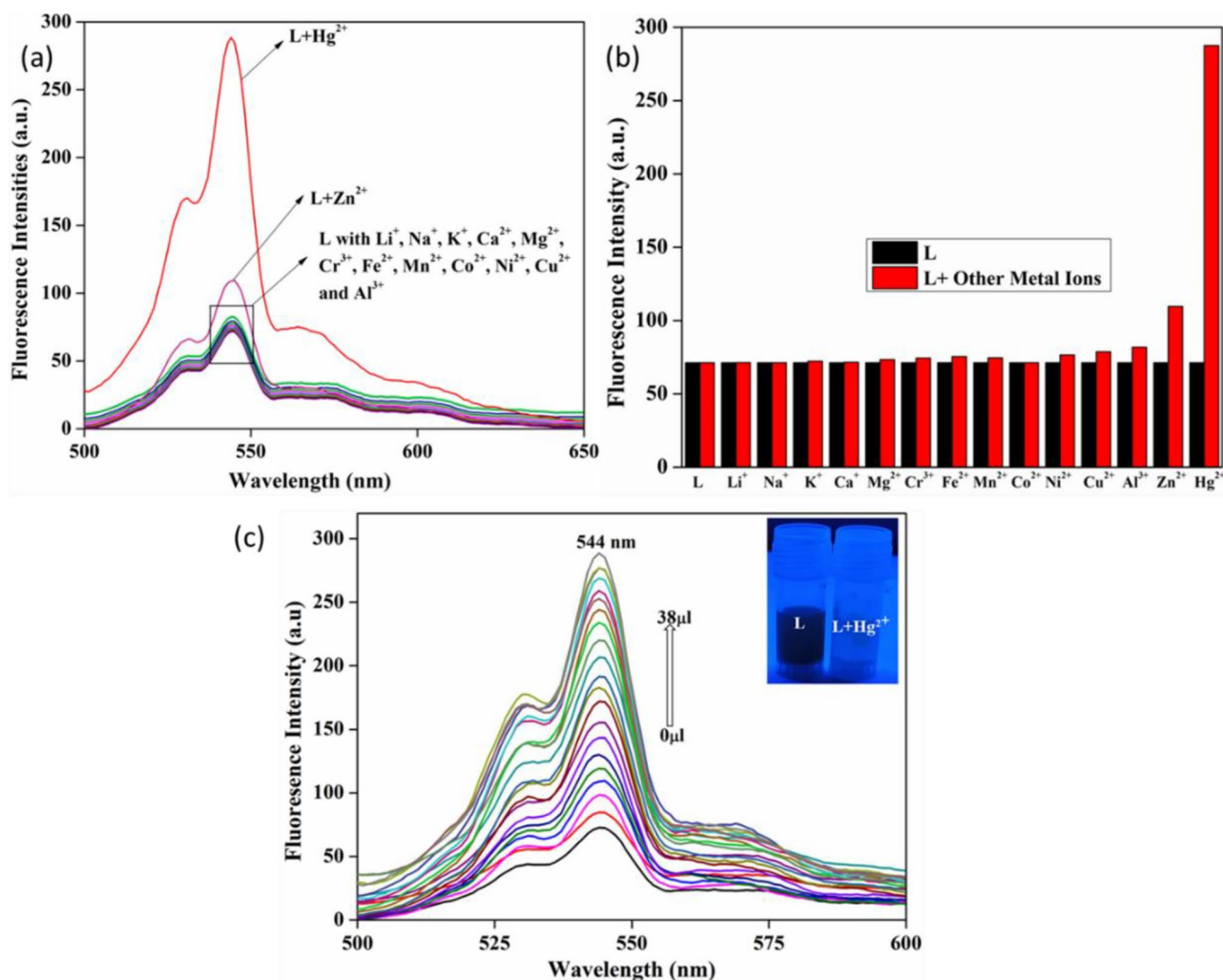


Fig. 3 **a** Fluorescence spectra of **L** (2000 μL , 10^{-5} M) in DMSO upon the incorporation of various metal ions (2 μL in each aliquot). **b** Bar diagram of **L** fluorescence intensities at 544 nm in the absence and

presence of various metal ions. **c** Fluorescence emission intensity of **L** that changes when Hg^{2+} ions are added gradually (0–38 μL , 10^{-5} M)

(Insert in Fig. 2b). The results clearly delineated that receptor **L** can be utilized for the selective and sensitive detection of Hg^{2+} . To provide further information regarding the binding affinity of the receptor towards Hg^{2+} , fluorescence selectivity and titration experiments are performed [35].

Fluorescence Sensing Behavior of **L**

To further explore the selectivity of **L** towards Hg^{2+} , a fluorescence selectivity experiment was carried out in DMSO. The molecular probe **L** in DMSO solution generates a weak fluorescent emission peak at 544 nm when excited at 410 nm. The weak emission intensity of **L** at 544 nm may be caused by the intermolecular charge transfer of electrons [36]. With the addition of several metal ions such as Na^+ , Mn^{2+} , Li^+ , Ni^{2+} , Fe^{2+} , Cr^{3+} , Ca^{2+} , K^+ , Mg^{2+} , Co^{2+} , Cu^{2+} , Zn^{2+} , Al^{3+} and Hg^{2+} no such noticeable alteration in spectral behavior was observed except for Hg^{2+} (Fig. 3a). In the presence of Hg^{2+} , the fluorescence intensity of **L** increased significantly at 544 nm (Fig. 3b). Further titration experiments of Hg^{2+} against the DMSO solution of **L** were carried out

to provide evidence in favor of the selectivity of **L** towards Hg^{2+} . The incremental addition of Hg^{2+} ($2 \mu\text{L}$ in each aliquot, 10^{-5} M) to the DMSO solution of **L** results in a gradual enhancement of emission intensity at 544 nm (Fig. 3c). The non-fluorescent **L** changed to a light blue fluorescent in the presence of Hg^{2+} (Insert in Fig. 3c). The fluorescence emission intensity of **L** was increased gradually, with a little red-shift with the incremental addition of Hg^{2+} . The change in spectral behavior and alteration in color provide evidence of interaction between **L** and Hg^{2+} .

Sensing Mechanism

To comprehend the mechanism of interaction between chromone-based Schiff base **L** and Hg^{2+} , the Benesi-Hildebrand plot was plotted using the fluorescence titration data [37]. The binding constant K_a for the **L**- Hg^{2+} complex was evaluated graphically using the Benesi-Hildebrand plot (Fig. 4a) [38]. The linear fit plot from the Benesi-Hildebrand plot indicates a 1:1 stoichiometry for the complexation occurring between **L** and Hg^{2+} [39]. Using the B-H equation [40], the K_a of

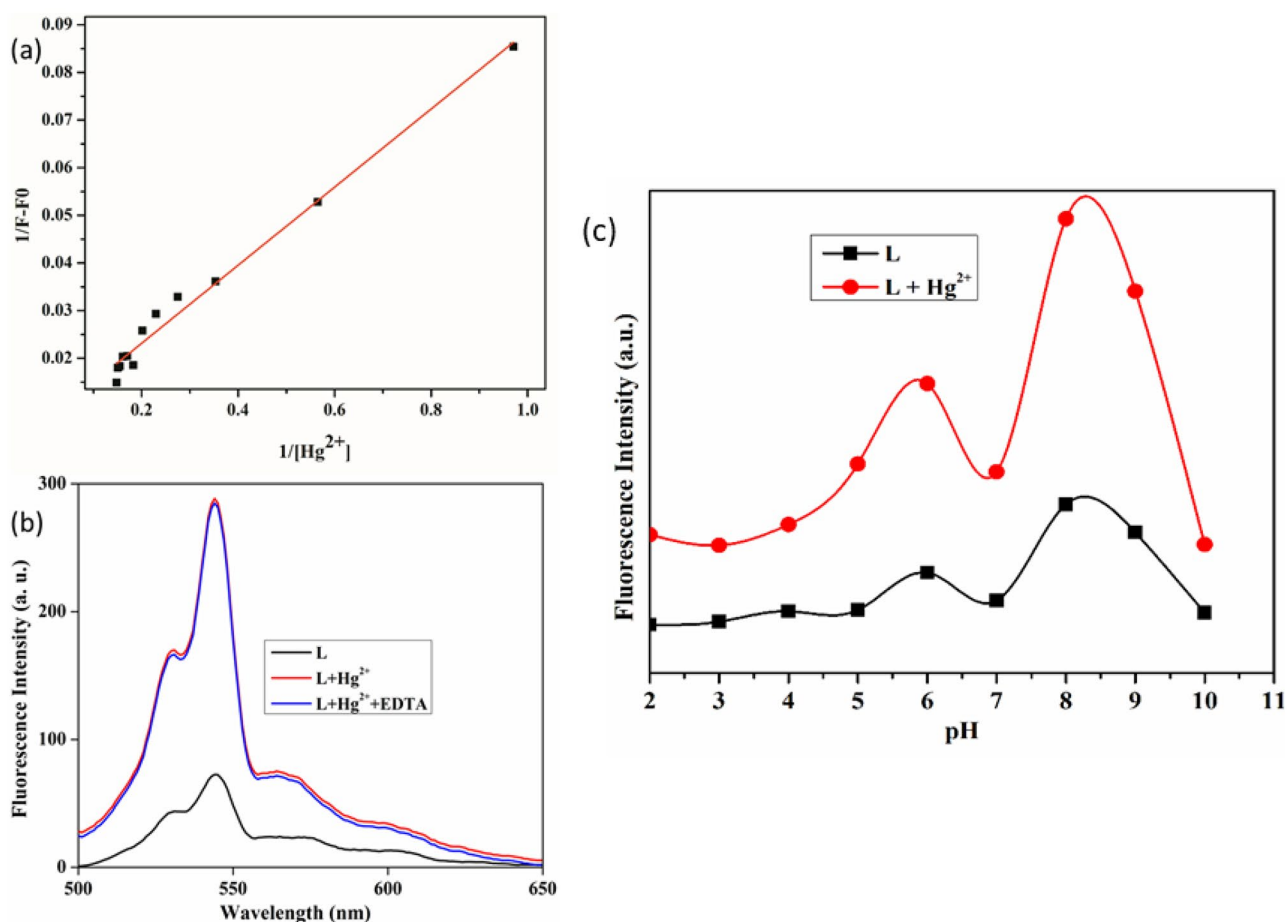


Fig. 4 **a** Benesi-Hildebrand plot. **b** Reversibility of **L** against Hg^{2+} in presence of sodium salt of EDTA. **c** Effect of different pH on the fluorescence changes of **L** in the absence and presence of Hg^{2+} ion

Table 1 Comparison of the characteristics of the proposed ligand with previous reported literature

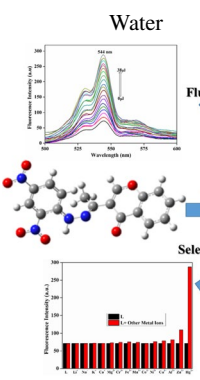
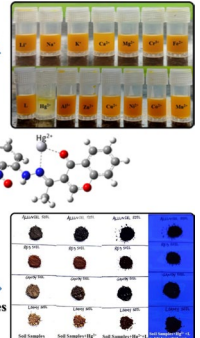
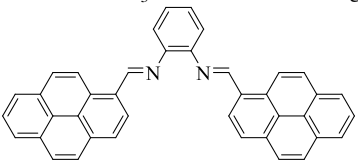
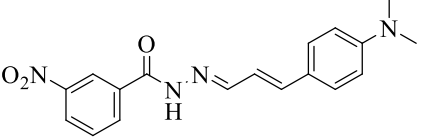
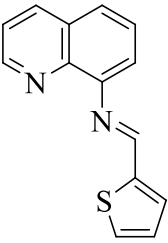
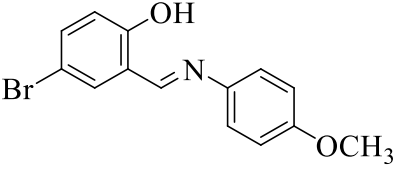
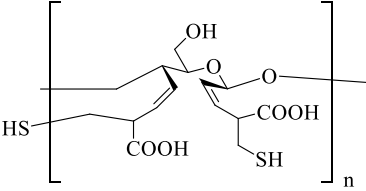
Receptors	Medium	Metal ions	Detection limit (M)	Binding Constant (M ⁻¹)	Application	Ref.
	Water	Hg ²⁺	0.34×10^{-6}	1.7×10^4	Paper strip sensor	42
		Soil Samples	Hg ²⁺			
	CH ₃ OH	Hg ²⁺	9.0×10^{-8}	1.15×10^4	Cell imaging and test strip application	43
	DMF	Hg ²⁺	0.11×10^{-4}	2.0×10^3	Real sample analysis	44
	HEPES buffer solution	Hg ²⁺	2.34×10^{-8}	5.27×10^4	Cell Imaging and Paper strip application	45
	THF	Hg ²⁺	3.98×10^{-8}	***	Real sample analysis	46
	Phosphate Buffer	Hg ²⁺	4.093×10^{-5}	***	Real sample analysis	47

Table 1 (continued)

Receptors	Medium	Metal ions	Detection limit (M)	Binding Constant (M ⁻¹)	Application	Ref.
	DMSO/PBS buffer	Hg ²⁺	0.022 × 10 ⁻⁶	2.23 × 10 ¹³	Cell imaging and test paper	48
	Ethanol	Hg ²⁺	0.26 × 10 ⁻⁶	7.35 × 10 ¹¹	Environmental Sample and Biological Studies	49
	HEPES buffer solution	Hg ²⁺	2.7 × 10 ⁻⁸	1.2 × 10 ⁵	Detection of mercury in Urine sample	50
	DMSO	Hg ²⁺	1.870 × 10 ⁻⁶	1.234 × 10 ⁷	Detection of Mercury in Soil sample	Present Work

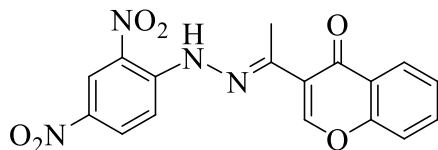
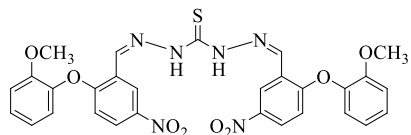
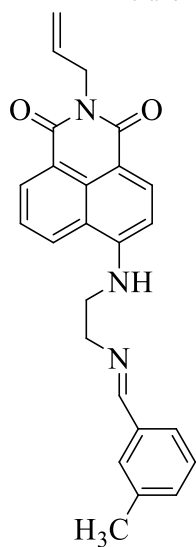
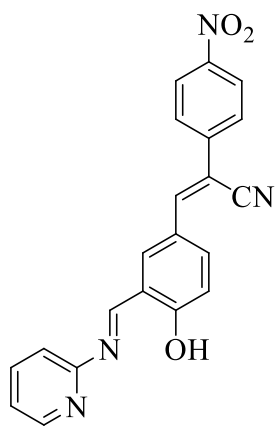


Fig. 5 FTIR spectra of **L** in the absence and presence of Hg^{2+}

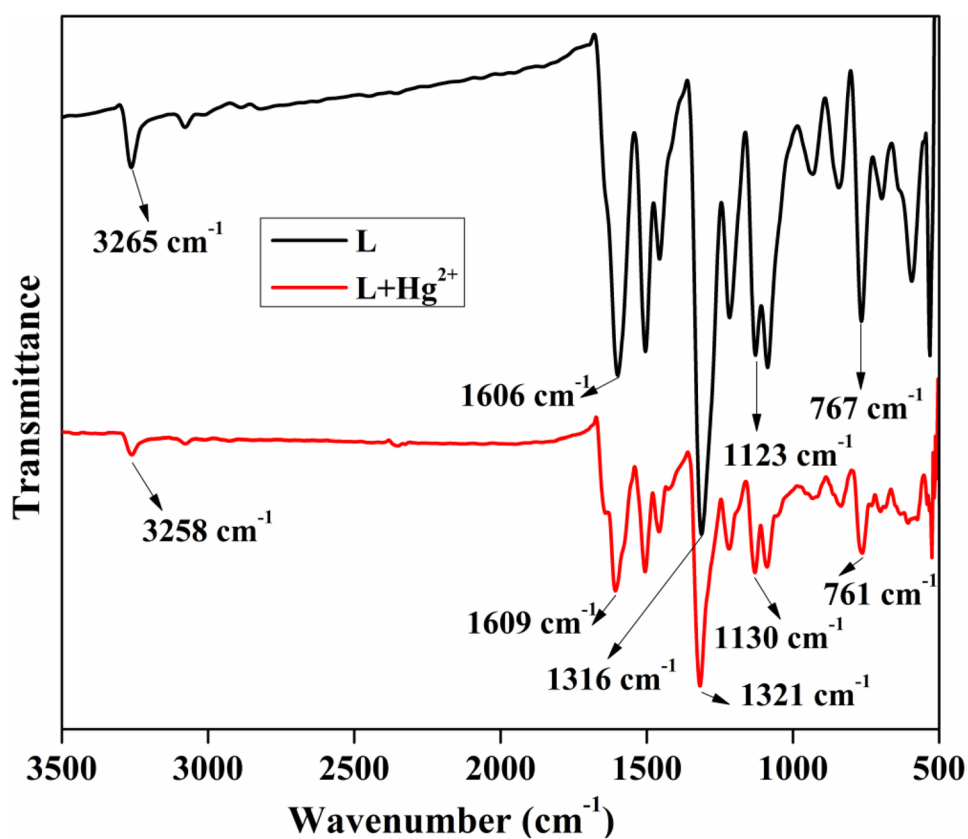
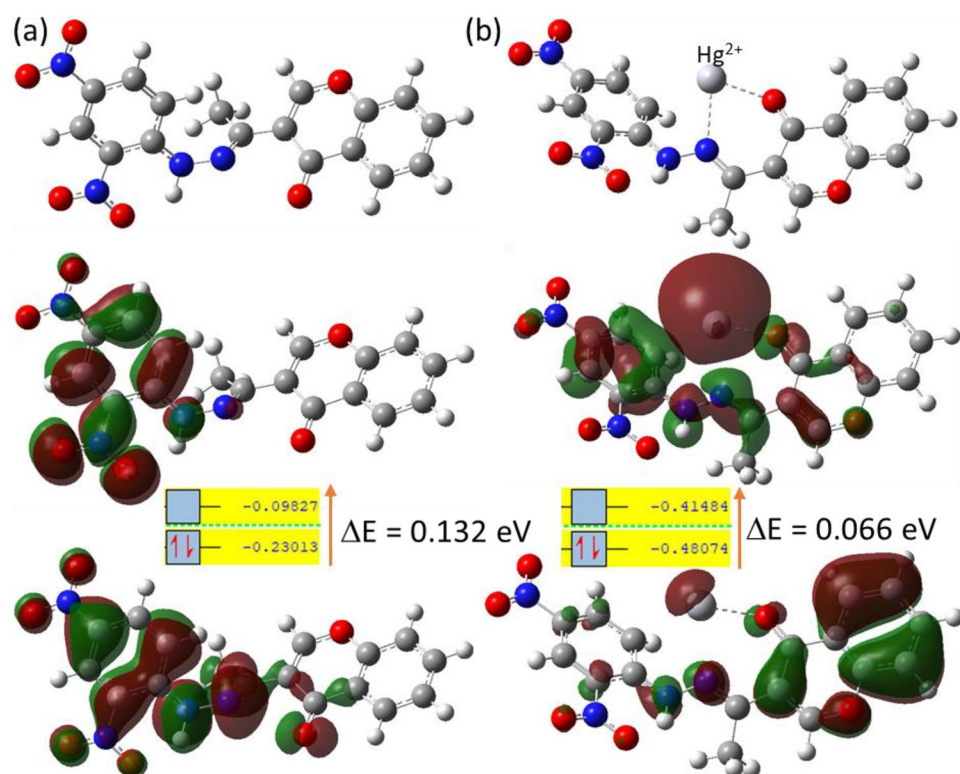


Fig. 6 DFT (B3LYP/6-31G**/LANL2DZ) computed 3D structure of **L** (a) and **L-Hg²⁺** complex with their LUMO and HOMO diagrams



receptor **L** with Hg^{2+} was determined as $1.234 \times 10^7 \text{ M}^{-1}$. The limit of detection for Hg^{2+} was also calculated to be $1.870 \times 10^{-6} \text{ M}$, which is found to be very much lower than that of the reported probes (Table 1).

To investigate the reversibility behavior of **L**, the reversibility test of **L** against Hg^{2+} was implemented in the presence of the disodium salt of EDTA. The **L** in DMSO solution results in a weak emission peak at 544 nm (Fig. 4b). The addition of Hg^{2+} (38 μL) resulted in an enormous increase in the fluorescence emission peak at 544 nm. But it was astonishing to note that the addition of EDTA, even if in excess, didn't show any alteration in fluorescence intensity. Even in the presence of EDTA, the color of the complex solution didn't recovered. The results clearly indicated that the complex of **L** and Hg^{2+} is irreversible in nature. The irreversibility supported the high stability of the **L**- Hg^{2+} complex formed in solution. The effects of pH on the fluorescence sensing of Hg^{2+} by **L** was examined from pH 2 to 10 (Fig. 4c). Schiff base **L** can be employed for the detection of Hg^{2+} over a wide pH range [41].

The FTIR study was performed to examine the interaction that occurred between **L** and Hg^{2+} . The FTIR spectrum

of **L** resulted in peaks at 3265 cm^{-1} and 1606 cm^{-1} due to $-\text{NH}$ stretching vibration and $-\text{C}=\text{N}$ vibration, respectively (Fig. 5). It is observed that in the FTIR spectrum of the **L**- Hg^{2+} complex, the $-\text{NH}$ vibration peak and $-\text{C}=\text{N}$ vibration peak shifted to 3258 and 1609 cm^{-1} , respectively. It clearly signifies that the azomethine group participates in the interaction of **L** with Hg^{2+} . The other peaks of **L** at 1316 , 1123 and 767 cm^{-1} of $-\text{NO}_2$, $-\text{C}-\text{O}$ and mono-substituted $\text{C}-\text{H}$ bending respectively shift to 1321 , 1130 and 761 cm^{-1} in the presence of Hg^{2+} , which also indicates the complexation occurred between **L** and Hg^{2+} .

The density functional theory (DFT) calculations were performed using B3LYP exchange-correlation functional B3LYP to obtain the 3D structure of the Schiff base **L** and **L**- Hg^{2+} complexes in the gas phase [42]. The basis sets LANL2DZ for the Hg atom whereas 6-31G** for C, H, O and N atoms were used for the calculations by using the computational programme Gaussian 09 W [43]. The computed structures of the Schiff bases **L** and **L**- Hg^{2+} are shown in Fig. 6. In solution, the conformational flexibility at the $-\text{C}=\text{N}$ linkage, along with the photo-induced electron transfer (PET) process [44], is expected to quench

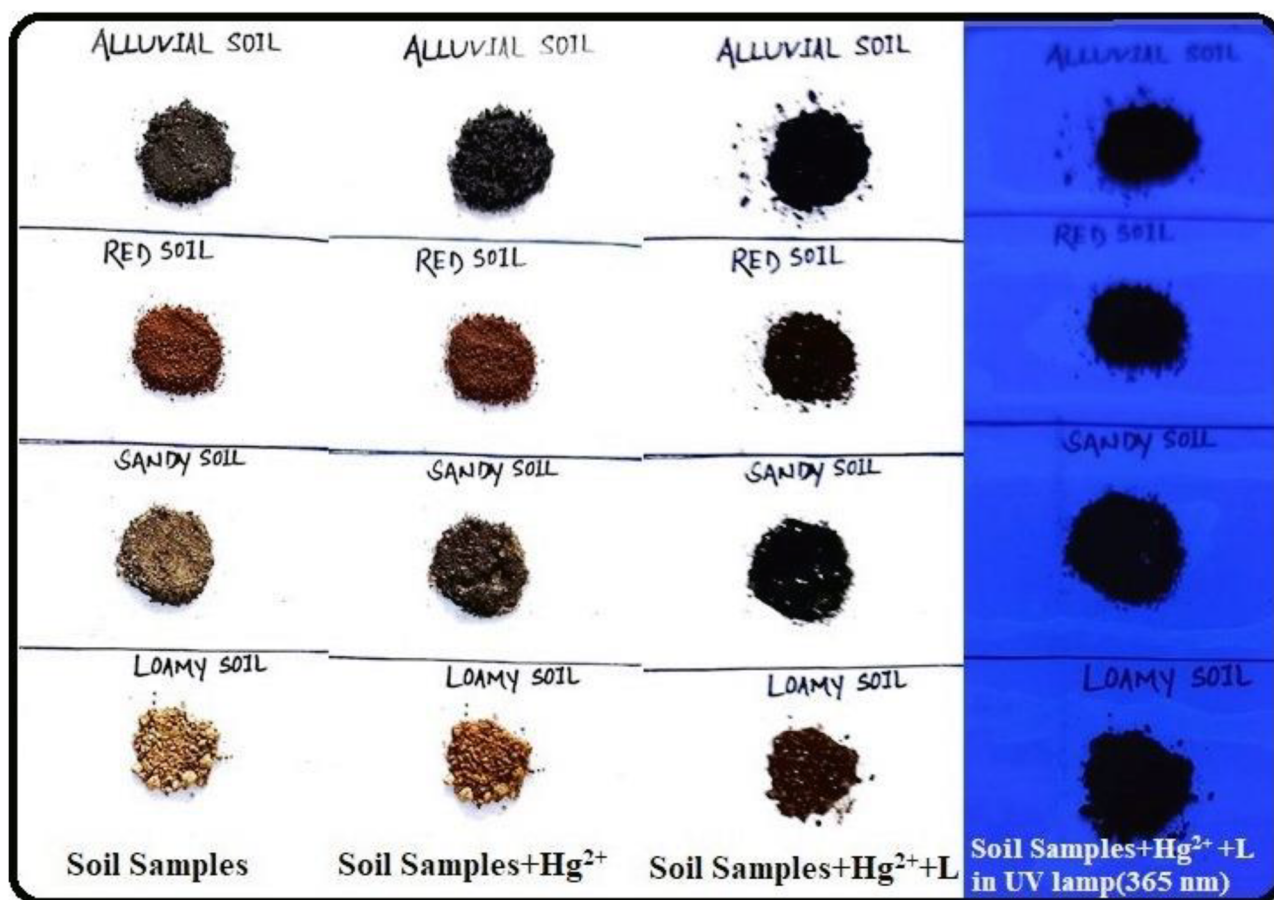


Fig. 7 Recognition of Hg^{2+} in various soil samples: **a** in naked-eye without ligand, **b** in naked-eye with Hg^{2+} , **c** in naked-eye with Hg^{2+} and **L** **d** in UV-lamp at 365 nm with ligand

the fluorescence emission of **L**. Schiff base **L** provides an ideal bidentate coordination environment through imine-N and formyl chromone-O donor atoms to chelate Hg^{2+} . With the formation of the L-Hg^{2+} complex, the DFT-computed interaction energy ($E_{\text{int}} = E_{\text{complex}} - E_{\text{receptor}} - E_{\text{Hg}^{2+}}$) got lowered by -214.57 kcal/mol, supporting the formation of a stable and favourable complex between **L** and Hg^{2+} . The formation of the L-Hg^{2+} complex also lowered the band gap between the lowest unoccupied molecular orbital (LUMO) and the highest occupied molecular orbital (HOMO) [45]. Further analysis of the HOMO and LUMO electron densities of the **L** and L-Hg^{2+} complexes revealed that charge transfer occurred from the ligand to the Hg^{2+} metal ions. Therefore, the complexation-induced inhibition of PET and $\text{C}=\text{N}$ isomerization is responsible for the fluorescence switch-on response from **L** upon interaction with Hg^{2+} [46].

Real Sample Analysis

The Hg^{2+} detection ability of Schiff base probe **L** was investigated under various nutrient soil samples [47]. The soil samples have a profound role in the field of agriculture [48]. The soil samples, like alluvial soil, red soil, sandy soil and loamy soil full of nutrients are collected from nearby agricultural areas of Veer Surendra Sai University of Technology Burla, Sambalpur, and Odisha [49]. All the collected soil samples are poured with Hg^{2+} solution. The addition of Hg^{2+} results in a small alteration in the color of the solution to the naked-eye. Further, with the addition of DMSO/ H_2O (90:10, v/v) solution of **L** to the mercury-containing soil samples, the color of the solution becomes darkened in the naked-eye [50]. This alteration was also observed under the UV lamp at 365 nm (Fig. 7). The results suggested that the receptor **L** can detect Hg^{2+} in real samples.

Conclusions

A novel formyl-chromone-based chromofluorogenic sensor **L** was successfully developed and characterized by various spectral techniques. The receptor **L** exhibited good sensitivity and selectivity towards Hg^{2+} over other competing species in DMSO/ H_2O (10:90, v/v) solution. In the presence of Hg^{2+} , receptor **L** showed a decrease in the absorption intensity at 396 nm and an increment in the fluorescence emission intensity at 544 nm. In the presence of Hg^{2+} , the receptor **L** also displayed naked-eye detectable colour change under day and UV light upon complexation with Hg^{2+} in a 1:1 binding ratio. Using the fluorescence titration data, the detection limit and binding constant of **L** for Hg^{2+} were found to be 1.870×10^{-6} M and 1.234×10^7 M^{-1} , respectively. Finally,

receptor **L** was successfully applied for the qualitative detection of Hg^{2+} ions in various soil samples.

Supplementary Information The online version contains supplementary material available at <https://doi.org/10.1007/s10895-023-03500-z>.

Author Contributions All authors contributed to the study: The Investigation, Validation, Formal analysis, Data curation, Writing-original draft were performed by Soumya Ranjan Kar, Pragyana Parimita Dash, Sankalpa Narayan Panda, Patitapaban Mohanty, Debasis Mohanty, Aruna Kumar Barick. The Conceptualization, Resources, Supervision, and Writing-review & editing were performed by Priyaranjan Mohapatra, Suban Kumar Sahoo and Bigyan Ranajn Jali.

Funding Dr. Jali acknowledges a fund from DST-Biotechnology, Govt. of Odisha, and Project No.: ST-BT-MISC-0008-2020-245/ST, dated 12-01-2022. The authors also thank to Department of Chemistry, VSSUT, Burla, SVNIT Surat and Dhenkanal (Auto) College, Dhenkanal, Odisha for providing research facility.

Data Availability All data generated during this study are included in this published article.

Declarations

Ethics Approval Not applicable as the study does not include any use of animals and humans.

Consent to Participate Not applicable.

Consent to Publish Not applicable.

Competing Interests The authors declare no competing interests.

References

1. Wu D, Sedgwick AC, Gunnlaugsson T, Akkaya EU, Yoon J, James TD (2017) Fluorescent chemosensors: the past, present and future. *Chem Soc Rev* 46:7105–7123. <https://doi.org/10.1039/C7CS00240H>
2. Jali BR (2021) A Mini-review: Quinones and their derivatives for selective and Specific Detection of Specific Cations. *Biointerface Res Appl Chem* 11:11679–11699. <https://doi.org/10.33263/BRIAC114.1167911699>
3. Udhayakumari D, Inbaraj V (2020) A review on Schiff base fluorescent chemosensors for cell imaging applications. *J Fluoresc* 30:1203–1223. <https://doi.org/10.1007/s10895-020-02570-7>
4. Devi J, Batra N (2015) Synthesis, characterization and antimicrobial activities of mixed ligand transition metal complexes with isatin monohydrazone schiffbase ligands and heterocyclic nitrogen base. *Spectrochimica Acta Part A: Mol Biomol Spectrosc* 135:710–719. <https://doi.org/10.1016/j.saa.2014.07.041>
5. Mohanty P, Behura R, Bhardwaj V, Dash PP, Sahoo SK, Jali BR (2022) Recent advancement on chromo-fluorogenic sensing of aluminum (III) with Schiff bases. *Trends Environ Anal Chem* 34:e00166. <https://doi.org/10.1016/j.teac.2022.e00166>
6. Ahlawat A, Khatkar P, Singh V, Asija S (2018) Diorganotin (IV) complexes of Schiffbases derived from salicylaldehyde and 2-amino-6-substituted benzothiazoles: synthesis, spectral studies, and in vitro antimicrobial evaluation and QSAR studies. *Res Chem Intermediates* 44:4415–4435. <https://doi.org/10.1007/s11164-018-3395-z>
7. Liu CJ, Yang ZY, Fan L, Jin XL, An JM, Cheng XY, Wang BD (2015) Novel optical selective chromone Schiff base chemosensor

- for Al^{3+} ion. *J Lumin* 158:172–175. <https://doi.org/10.1016/j.jlumin.2014.09.037>
8. Dash PP, Patel DA, Mohanty P, Behura R, Behera S, Sahoo SK, Jali BR (2023) Advances on chromo-fluorogenic sensing of copper (II) with Schiff bases. *Inorganica Chim Acta* 556:121635. <https://doi.org/10.1016/j.ica.2023.121635>
 9. Park JD, Zheng W, Prev J (2012) Human exposure and health effects of inorganic and elemental mercury. *Med Public Health* 45:344–352. <https://doi.org/10.3961/jpmph.2012.45.6.344>
 10. Tchounwou PB, Yedjou CG, Patlolla AK, Sutton D (2012) Heavy metal toxicity and the Environment. *Heavy metal toxicity and the environment. Mol Clin Environ Toxicol* 3:133–164. https://doi.org/10.1007/978-3-7643-8340-4_6
 11. Olivieri G, Novakovic M, Savaskan E, Meier F, Baysang G, Brockhaus M, Mullerspahn F (2002) The effects of β -estradiol on SHSY5Y neuroblastoma cells during heavy metal induced oxidative stress, neurotoxicity and β -amyloid secretion. *Neurosci* 113:849–855. [https://doi.org/10.1016/S0306-4522\(02\)00211-7](https://doi.org/10.1016/S0306-4522(02)00211-7)
 12. Lebel J, Mergler D, Lucotte M, Amorim M, Dolbec (1998) Neurotoxic effects of low-level methylmercury contamination in the Amazonian Basin. *Environ Res* 79:20–32. <https://doi.org/10.1006/enrs.1998.3846>
 13. Vimercati L, Santarelli L, Pesola G, Drago I, Lasorse G, Valentino M, Vacca A, Soleo L (2001) Monocyte-macrophage system and polymorphonuclear leukocytes in workers exposed to low levels of metallic mercury. *Sci Total Environ* 270:157–163. [https://doi.org/10.1016/S0048-9697\(00\)00780-4](https://doi.org/10.1016/S0048-9697(00)00780-4)
 14. Bloom N, Fitzgerald W (1998) Determination of volatile mercury species at the picogram level by low-temperature gas chromatography with cold-vapour atomic fluorescence detection. *Anal Chim Acta* 208:151–161. [https://doi.org/10.1016/S0003-2670\(00\)80743-6](https://doi.org/10.1016/S0003-2670(00)80743-6)
 15. Mohanty P, Dash PP, Naik S, Behura R, Mishra M, Sahoo H, Sahoo SK, Barick AK, Jali BR (2023) A thiourea-based fluorescent turn-on chemosensor for detecting Hg^{2+} , Ag^{+} and Au^{3+} in aqueous medium. *J Photochem Photobiol A: Chem* 437:114491. <https://doi.org/10.1016/j.jphotochem.2022.114491>
 16. Zhang Z, Zhang B, Qian X, Li Z, Xu Z, Yang Y (2014) Simultaneous quantification of Hg^{2+} and MeHg^{+} in aqueous media with a single fluorescent probe by Multiplexing in the Time Domain. *Anal Chem* 86:11919–11924. <https://doi.org/10.1021/ac503900w>
 17. Jiang W, Wang W (2009) A selective and sensitive turn-on fluorescent chemodosimeter for Hg^{2+} in aqueous media via Hg^{2+} promoted facile desulfurization–lactonization reaction. *Chem Commun* 3913–3915. <https://doi.org/10.1039/B903606G>
 18. Yang YK, Yook KJ, Tae J (2005) A rhodamine-based fluorescent and colorimetric chemodosimeter for the Rapid detection of Hg^{2+} ions in aqueous media. *J Am Chem Soc* 127:16760–16761. <https://doi.org/10.1021/ja054855t>
 19. Khan S, Chen X, Almahri A, Allehyani ES, Alhumaydhi FA, Ibrahim MM, Ali S (2021) Recent developments in fluorescent and colorimetric chemosensors based on Schiff bases for metallic cations detection: a review. *J Environ Chem Eng* 9(6):106381. <https://doi.org/10.1016/j.jece.2021.106381>
 20. Curdova E, Vavruskova L, Suchanek M, Baldrian P, Gabriel J (2004) ICP-MS determination of heavy metals in submerged cultures of wood-rotting fungi. *Talanta* 62:483–487. <https://doi.org/10.1016/j.talanta.2003.08.030>
 21. Gasparik J, Vladarova D, Capcarova M, Smehyl P, Slamecka J, Garaj P, Massanyi P (2010) Concentration of lead, cadmium, mercury and arsenic in leg skeletal muscles of three species of wild birds. *J Environ Sci Health A* 45:818–823. <https://doi.org/10.1080/10934521003708992>
 22. Pohl P (2009) Determination of metal content in honey by atomic absorption and emission spectrometries. *Trend Anal Chem* 28:117–128. <https://doi.org/10.1016/j.trac.2008.09>
 23. Flamini R, Panighel A (2006) Mass spectrometry in grape and wine chemistry. Part II: the consumer protection. *Mass Spectr Rev* 25:741–774. <https://doi.org/10.1002/mas.20087>
 24. Bothra S, Solanki JN, Sahoo SK (2013) Functionalized silver nanoparticles as chemosensor for pH, Hg^{2+} and Fe^{3+} in aqueous medium. *Sens Actuators B: Chem* 188:937–943. <https://doi.org/10.1016/j.snb.2013.07.111>
 25. Hoang LTA, Nguyen TC, Pham HY, Nguyen XN, Bui HT, Do TT, Nguyen HN, Van CM, Van PK, Young HK (2015) Promising anticancer drug candidates based on the 7-methoxychromone scaffold: synthesis and evaluation of antiproliferative activity. *Lett Drug Des Discov* 12:385–392. <https://doi.org/10.2174/1570180812666141111235539>
 26. Manjunath R, Hrishikesan E, Kannan P (2015) A selective colorimetric and fluorescent sensor for Al^{3+} ion and its application to cellular imaging. *Spectrochim Acta Part A Mol Biomol Spectrosc* 140:509–515. <https://doi.org/10.1016/j.saa.2015.01.015>
 27. Amalraj A, Pius A (2015) Chemosensor for fluoride ion based on chromone. *J Fluor Chem* 178:73–78. <https://doi.org/10.1016/j.jfluchem.2015.07.001>
 28. Malkondou S (2014) A highly selective and sensitive perylenebisimidebased fluorescent PET sensor for Al^{3+} determination in MeCN. *Tetrahedron* 70:5580–5584. <https://doi.org/10.1016/j.tet.2014.06.094>
 29. Feng XJ, Tian PZ, Xu Z, Chen SF, Wong MS (2013) Fluorescence-enhanced Chemosensor for Metal Cation Detection based on pyridine and Carbazole. *Org Chem* 78(22):11318–11325. <https://doi.org/10.1021/jo401808c>
 30. Behura R, Dash PP, Mohanty P, Behera S, Mohanty M, Dinda R, Behera SK, Barick AK, Jali BR (2022) A Schiff base luminescent chemosensor for selective detection of Zn^{2+} in aqueous medium. *J Mol Struct* 1264:133310. <https://doi.org/10.1016/j.molstruc.2022.133310>
 31. Behura R, Mohanty P, Sahu G, Dash PP, Behera S, Dinda R, Hota PR, Sahoo H, Bhaskaran R, Barick AK, Mohapatra P, Jali BR (2023) A highly selective Schiff base fluorescent sensor for Zn^{2+} , Cd^{2+} and Hg^{2+} based on 2, 4-dinitrophenylhydrazine derivative. *Inorg Chem Commun* 154:110959. <https://doi.org/10.1016/j.inoche.2023.110959>
 32. Behura R, Behera S, Mohanty P, Dash PP, Panigrahi R, Mallik BS, Sahoo SK, Jali BR (2022) Fluorescent sensing of water in DMSO by 2, 4-dinitrophenyl hydrazine derived Schiff base. *J Mol Struct* 1251:132086. <https://doi.org/10.1016/j.molstruc.2021.132086>
 33. David CI, Bhuvanesh N, Jayaraj H, Thamilselvan A, Devi DP, Abiram A, Prabhu J, Nandhakumar R (2020) Experimental and theoretical studies on a simple S–S-bridged dimeric schiff base: selective chromo-fluorogenic chemosensor for nanomolar detection of Fe^{2+} & Al^{3+} ions and its varied applications. *ACS Omega* 5(6):3055–3072. <https://doi.org/10.1021/acsomega.9b04294>
 34. Gusev AN, Kiskin MA, Braga EV, Chapran M, Wiosna-Salyga G, Baryshnikov GV, Minaeva VA, Minaev BF, Ivaniuk K, Stakhira P, Agren H (2019) Novel zinc complex with an ethylenediamine Schiff base for high-luminance blue fluorescent OLED applications. *J Phys Chem C* 123(18):11850–11859. <https://doi.org/10.1021/acs.jpcc.9b02171>
 35. Ellis GP (1977) Analytical aspects of Chromones. *Chem Heterocycl Compd* 31:1–10. <https://doi.org/10.1002/9780470187012.ch8>
 36. Pan X, Jiang J, Li J, Wu W, Zhang J (2019) Theoretical design of near-infrared Al^{3+} fluorescent probes based on salicylaldehyde acylhydrazone schiff base derivatives. *Inorg Chem* 58(19):12618–12627. <https://doi.org/10.1021/acs.inorgchem.9b01335>
 37. Sidana N, Devi P, Kaur H (2022) Thiophenol amine-based Schiff base for colorimetric detection of Cu^{2+} and Hg^{2+} ions. *Opt Mater* 124:111985. <https://doi.org/10.1016/j.optmat.2022.111985>
 38. Prakash A, Malhotra R (2018) Co(II), ni(II), Cu(II) and zn(II) complexes of aminothiazole-derived Schiff base ligands: synthesis, characterization, antibacterial and cytotoxicity evaluation,

- bovine serum albumin binding and density functional theory studies. *Appl Organomet Chem* 32(2):e4098. <https://doi.org/10.1002/aoc.4098>
39. Rathod RV, Bera S, Maity P, Mondal D (2020) Mechanochemical synthesis of a fluorescein-based sensor for the selective detection and removal of Hg^{2+} ions in industrial effluents. *ACS Omega* 5(10):4982–4990. <https://doi.org/10.1021/acsomega.9b03885>
40. Chethanakumar BM, Gudasi KB, Vadavi RS, Bhat SS (2023) Luminescent pyrene-based Schiff base receptor for Hazardous Mercury (II) detection demonstrated by cell imaging and test Strip. *J Fluoresc* 33(2):539–551. <https://doi.org/10.1007/s10895-022-03066-2>
41. Alorabi AQ, Mohamed M, Zabin SA (2020) Colorimetric detection of multiple metal ions using schiffbase 1-(2-Thiophenylimino)-4-(N-dimethyl) benzene. *Chemosensors* 8(1):1. <https://doi.org/10.3390/chemosensors8010001>
42. Mondal B, Banerjee S, Ray J, Jana S, Senapati S, Tripathy T (2020) Novel dextrin-cysteine Schiff Base: a highly efficient sensor for Mercury ions in Aqueous Environment. *Chem Select* 5(6):2082–2093. <https://doi.org/10.1002/slct.201904351>
43. Qiu J, Jiang S, Lin B, Guo H, Yang F (2019) An unusual AIE fluorescent sensor for sequentially detecting Co^{2+} - Hg^{2+} - Cu^{2+} based on diphenylacrylonitrile Schiff-base derivative. *Dyes Pig* 170:107590. <https://doi.org/10.1016/j.dyepig.2019.107590>
44. Wu HL, Dong JP, Sun FG, Li RX, Jiang YX (2022) New Selective fluorescent Turn-On Sensor for detection of Hg^{2+} based on a 1, 8-Naphthalimide Schiff Base Derivative. *J Appl Spectrosc* 89(3):487–494. <https://doi.org/10.1007/s10812-022-01384-8>
45. Kumar A, Kumar D, Chhibber M (2020) Determination of Mercury ions in Aqueous Medium and urine sample using Thiocarbohydrazide based Sensor. *Chem Select* 5(43):13738–13747. <https://doi.org/10.1002/slct.202002914>
46. Alharthi SS, Fallatah AM, Al-Saidi HM (2021) Design and characterization of electrochemical sensor for the determination of mercury (II) ion in real samples based upon a new Schiff base derivative as an ionophore. *Sensors* 21(9):3020. <https://doi.org/10.3390/s21093020>
47. Musikavanhu B, Muthusamy S, Zhu D, Xue Z, Yu Q, Chiyumba CN, Mack J, Nyokong T, Wang S, Zhao L (2022) A simple quinoline-thiophene Schiff base turn-off chemosensor for Hg^{2+} detection: spectroscopy, sensing properties and applications. *Spectrochim Acta A Mol Biomol Spectrosc* 264:120338. <https://doi.org/10.1016/j.saa.2021.120338>
48. Kim A, Kim S, Kim C (2020) A conjugated Schiff base-based chemosensor for selectively detecting mercury ion. *J Chem Sci* 132:1–7. <https://doi.org/10.1007/s12039-020-01789-y>
49. Cummings RT, Dizio JP, Krafft GA (1988) Photoactivable fluorophores synthesis and photo activation of functionalized 3-aryl-2-(2-furyl)-chromones. *Tetrahedron Lett* 29:69–72. [https://doi.org/10.1016/0040-4039\(88\)80018-2](https://doi.org/10.1016/0040-4039(88)80018-2)
50. Ceramella J, Iacopetta D, Catalano A, Cirillo F, Lappano R, Sinicropi MS (2022) A review on the antimicrobial activity of Schiff bases: data collection and recent studies. *Antibiotics* 11(2):191. <https://doi.org/10.3390/antibiotics11020191>

Publisher's Note Springer Nature remains neutral with regard to jurisdictional claims in published maps and institutional affiliations.

Springer Nature or its licensor (e.g. a society or other partner) holds exclusive rights to this article under a publishing agreement with the author(s) or other rightsholder(s); author self-archiving of the accepted manuscript version of this article is solely governed by the terms of such publishing agreement and applicable law.